Romanian Reports in Physics, Vol. 63, No. 1, P. 61–75, 2011

NON-DESTRUCTIVE MEASUREMENT OF MOISTURE IN BUILDING MATERIALS BY COMPTON SCATTERING OF GAMMA RAYS

D. BUCURESCU[1,2], I. BUCURESCU[3]

[1]"Horia Hulubei" National Institute of Physics and Nuclear Engineering, R-76900 Bucharest, Romania, E-mail: bucurescu@tandem.nipne.ro
[2]Academy of Romanian Scientists, 54 Splaiul Independentei st., R-050094 Bucharest, Romania
[3]"Ion Mincu" University of Architecture and Urbanism, 18-20 Academiei st., R-010014 Bucharest, Romania, E-mail: iulia_bucurescu@yahoo.com

Received May 14, 2010

Abstract. A non-destructive method for measuring moisture within porous building materials is presented. It is based on the detection of the backward angle scattered gamma-rays of a ^{241}Am source, with a $LaBr_3$:Ce scintillator detector. An example of application of this method is given by measuring the moisture in bricks (building material) with various water contents. The method is suitable for the examination of building walls (houses, historical monuments) and of building material samples.

Key words: non-destructive measurement, moisture content, building materials, gamma-ray Compton scattering.

1. INTRODUCTION

The interplay between water and different materials is an important item in many fields. In particular, the water mediates most of the processes that cause the degradation and decay of the buildings. This is because many of the inorganic building materials, such as brick, stone, plaster, mortar, and concrete, are porous and absorb and transmit water through capillarity. Especially in the case of degraded historical monument buildings considered for restoration, it is important to detect the water infiltrations that lead to humidity of the walls above the normal limit and contribute to processes of physical, chemical, and biological degradation [1, 2].

Commonly used non-destructive, fast methods for the measurement of the moisture in walls, especially employed by the building professionals, such as those based on measuring different electrical characteristics of the surface (like resistance, impedance, capacitance, or dielectrical constant) record the presence of

the surface moisture, but are unable to determine the true moisture content within the wall. For such determinations, one usually recommends to collect samples from the wall and analyze them by specific methods (gravimetric or chemical) in the laboratory. This process may be lengthy and complicated in many cases, or even, in the case of historical monuments, not acceptable. Other non-destructive methods are therefore highly needed in such cases.

A large category of non-destructive methods is based on probing the medium by different radiations [3]. Thus, there are methods for the determination of moisture distribution within materials by neutron transmission [4], neutron backscattering [5] (see also other citations in [3]), or based on the NMR (nuclear magnetic resonance) [6, 7]. Without entering details of these techniques and of their advantages and disadvantages, we focus here on the methods based on the attenuation and scattering of the electromagnetic radiations (X or gamma-rays).

The interaction of the gamma rays with materials is a well understood process, and can be used to probe the inside of bulky objects, because they can penetrate at appreciable depths (of the order of several centimeters, depending on the material and on their energy). This interaction involves several processes, the most important for photons with energies up to several MeV being [3, 8]: the photoelectric effect (complete absorption of the energy of the photon by a bound atomic electron); coherent (or elastic) scattering (scattering by the atom as a whole, without loosing energy); incoherent (or Compton) scattering (by which the photon is scattered at a certain angle after giving part of its energy to an atomic electron); pair production (a photon of sufficient energy generates an electron-positron pair in the electromagnetic field of the nucleus). Many applications exploit the characteristics of the scattering processes. Of interest to us is that these processes take place on the electrons of the material, therefore they are sensitive to the density (mass density or electron density) of the irradiated material and can be used to determine density or changes of density (due to, e.g., voids, insertions of other materials, or water addition).

The attenuation of a beam of gamma rays that passes through a certain thickness of material depends on its density and elemental composition. Measuring this attenuation (by a transmission measurement, the radiation source and the detector being on opposite sides of the object) can be used to deduce, for example, the moisture content in soil [9, 10]. By measuring the attenuation of two gamma-rays which differ much in energy, one can simultaneously determine the water content and dry bulk density of the material [11, 12]. One should also mention the recent interest of measuring the attenuation of the gamma rays by building materials, aiming at the assessment of the houses' protection against outside radiations ([13–18] and other references quoted in these works).

The measurement of the gamma radiations Compton scattered by an object also provides density information. Unlike the attenuation (or transmission) method it does not require access to two opposite sides of the object, a fact that gives this

method an increased flexibility [3]. Consequently, the backscattering of the gamma rays found numerous applications, of which only a few will be cited (more examples can be found in [3]): in medicine, for the measurement of variations of density in bones, soft tissues, superficial organs [19, 20]; inspection of concrete structures [21, 22] or of off-shore structures (pipelines) [23]; inspection of corrosion in off-shore structures [24], or in aircraft [25, 26]; in surface inspection [27]. It also found many applications in the measurement of water content of soil [28–31].

In this work we present the application of the gamma ray Compton backscattering technique to the determination of moisture content in building materials, with a simple and compact experimental setup that lends itself to field applications.

2. EXPERIMENTAL SETUP

In the Compton scattering process, by which an incoming photon (gamma ray) is deflected by an angle θ with respect to its original direction after transferring a part of its energy to an electron, the energy of the scattered photon is given by [8]

$$E'_{\gamma} = \frac{E_{\gamma}}{1+\alpha(1-\cos\vartheta)}, \tag{1}$$

where $\alpha = E_{\gamma}/m_0c^2$, m_0c^2 = 511 keV is the rest mass of the electron, and E_{γ} the energy of the incident photon (the electron is assumed initially at rest). In order to use this relation the experimental setup should allow a clear measurement of this single scattering process. In many applications, both the radiation source and the detector are strongly collimated, such as the intersection of their fields-of-view defines a certain inspection (or sensitive) volume within the examined material [3] and a well defined scattering angle. One can relax one of the collimation conditions, usually that of the detector, if one measures the spectra with a detector of sufficiently good energy resolution, such that by selecting adequate regions of the spectra one makes sure that we consider only single scattering events, according to eq. (1). Such a detector may be a hyper-pure Germanium (HPGe) one, but the cost and the necessity of cooling it down to the liquid nitrogen temperature are factors that preclude its use in field applications. In our case we used a 2”×2” $LaBr_3$:Ce (lanthanum bromide doped with cerium) scintillator detector. The scintillator detectors with lanthanum bromide activated with cerium are new in the gamma-ray spectroscopy, and are being quickly adopted for a large variety of applications requiring detectors that operate at room temperature, due to their very good time resolution, good energy resolution, high efficiency, and fast decay time [32,33]. As we were just using such detectors in the laboratory for fast timing

spectroscopy, it was considered interesting to investigate their potential in other applications. The gamma-ray source used for these measurements was an available 0.385 GBq (10.4 mCi) ^{241}Am source. It emits a monoenergetic radiation of 59.54 keV. Because this is not a too high energy it does not need massive collimators/protection in order to define the geometry and remove the radiation hazard.

The experimental setup used in our final measurements is shown in Fig. 1. The ^{241}Am source, contained in a stainless steel cylinder of 3 mm diameter and 10 mm length, was placed within a hole drilled in a standard 5×10×10 cm lead brick, 5 mm diameter and 60 mm deep. This defined the gamma ray beam sent to be scattered by the examined object and protected the detector from gamma rays coming directly from the source. The scattered radiation was detected with the scintillator detector that was placed alongside the lead brick. The distance between the face of the detector and the surface of the investigated object was 8 cm. With an uncollimated detector, the present setup allows the detection of a relatively large range of angles for single scattering and also of multiple scattering events. Nevertheless, an examination of the conditions of measurement and of the quality of the spectra and their interpretation, will show that it is possible to extract the contribution of the single scattering events that originate in the interaction region around the gamma ray beam axis.

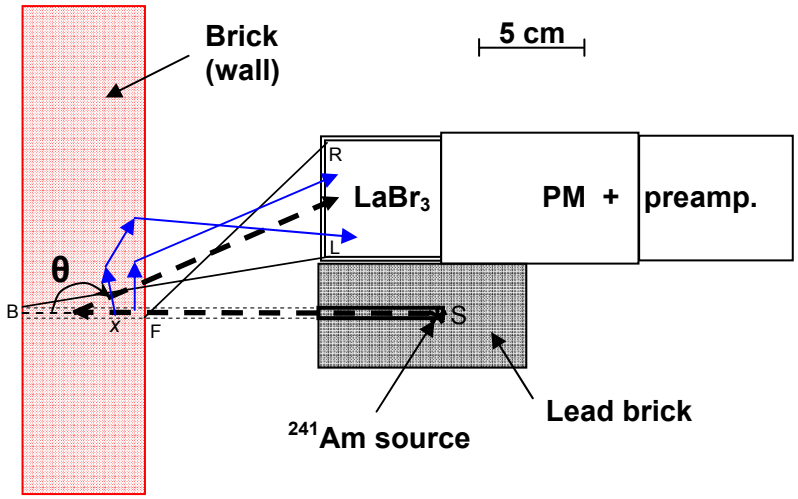

Fig. 1 – Sketch of the experimental setup used in the present measurements. Both sigle scattering and multiple-scattering processes are illustrated.

To demonstrate the feasibility of the method we performed measurements on a common building material, red fired-clay bricks. Figure 2 shows different gamma ray spectra, which were measured with a multichannel analyzer operating on a

laptop computer, in which the detector signals amplified with a linear amplifier were fed. One of the reported shortcomings of the $LaBr_3$:Ce scintillators is that they are slightly "self-active", due to the presence in their composition of some contaminants, among which the unstable isotope ^{138}La [32, 33]. Indeed, the spectrum in the upper panel in Fig. 2, measured without any source around the detector, shows one of the peaks due to this intrinsic activity, at 32 keV, representing the X-ray fluorescence of ^{138}Ba. The second panel (from top) in Fig. 2 shows a spectrum measured with a weak ^{241}Am source placed in front of the detector at a distance such as the 59.5 keV peak was comparable in intensity with the 32 keV one. It can be seen that in our case the presence of the weak 32 keV radiation may be considered an advantage, because it is close to the measured energies (below 60 keV) and can be used as a calibration point (also, because it is an intrinsic internal decay, it can be used for normalization purposes, its area being proportional to the measuring time). The FWHM energy resolution obtained in these measurements was 4.7 keV at 32 keV and 5.8 keV at 59.5 keV, respectively. This resolution is important for the processing and interpretation of the spectra. The two other spectra shown in the lowest panels of Fig. 2, show the radiation detected after scattering on bricks placed as in Fig. 1. The first spectrum was measured within a geometry slightly different from that in Fig. 1, in which the average scattering angle (that is, the angle between the gamma ray beam and a line which joins the point on the beam line in the center of the brick and the center of the detector) was about 100^0. The bottom spectrum was measured in the geometry of Fig. 1, where this average scattering angle is about 150^0. The strong peak seen in these spectra can be interpreted as mainly originating in single Compton scattering, as the energy of its maximum corresponds to what is expected for the average scattering angle according to eq. (1). Energy calibration of the spectra was made with sources of ^{133}Ba, ^{241}Am and ^{152}Eu. The bottom panels contain two spectra each, one measured with a "dry" brick, the other with a brick saturated with water (see discussion below). The effect of the water addition is an increased intensity of the Compton scattering peak. As already discussed, it is desirable to distinguish between events due to one Compton scattering, which obey eq. (1), and multiple Compton scattering events which can also be detected since our detector is completely open (Fig. 1). This will help to improve the sensitivity, because the stronger attenuation of the multiple-scattered photons (due to their lower energy) contributes to the deterioration of the scattering signal. Let us examine more closely the conditions of our measurements. From Fig. 1 we see that for single scattering events we measure a range of angles θ, from any point from the interaction region defined by the gamma ray beam to any point of the detector surface. The extreme angles are SBL (the angle approximately defined by the points S (the source), B (the point of the beam impact on the back of the brick) and

L (the "left" edge of the detector surface), and SFR (cf. same figure), which are of 169^0 and 133^0, respectively. The energies of the single scattered photons at these angles are 48.4 and 49.8 keV, respectively (compared to 48.9 keV corresponding to the "average" scattering angle of 150^0). The difference between the two extreme scattered energies is 1.4 keV, therefore detecting all one-scattering angles will only broaden the 48.9 keV peak by about this amount. Looking more closely at the bottom spectra in Fig. 2, one can observe that near the single Compton scattering peak the structure is more complicated. This is investigated in an example in Fig. 3, which shows the relevant part of a spectrum of the dry brick.

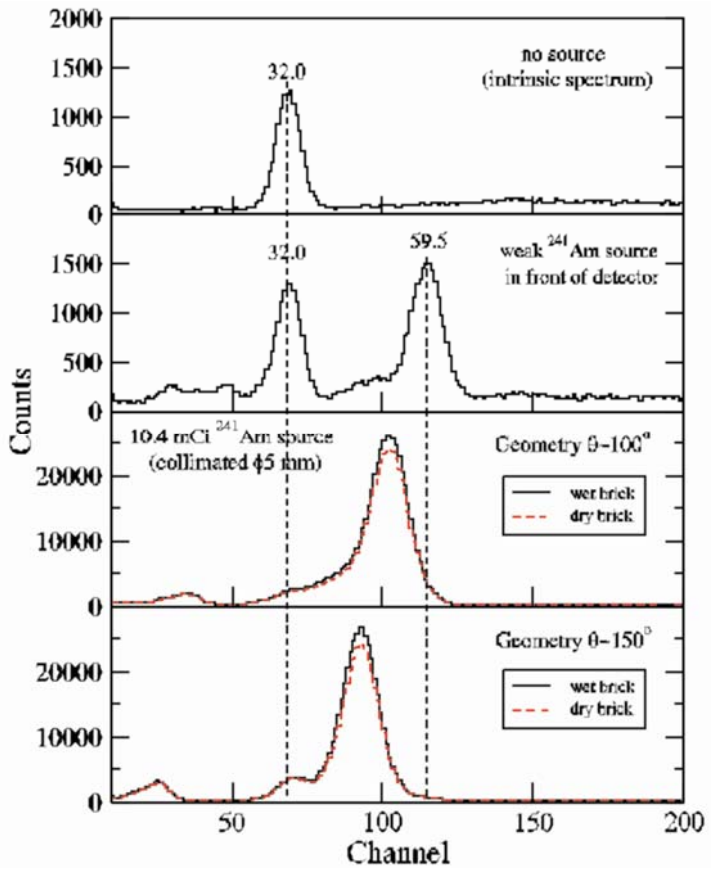

Fig. 2 – Region of the spectra obtained with the lanthanum bromide detector under different conditions. Upper graph: intrinsic spectrum of the detector. Second graph: weak ^{241}Am source in front of the detector. Third graph: spectra of the 59.5 keV radiation Compton scattered by both dry and wet brick, with an average scattering angle of 100^0. Bottom graph: spectrum of the 59.5 keV radiation Compton scattered on both dry and wet brick, in the geometry of Fig. 1 (average scattering angle of 150^0).

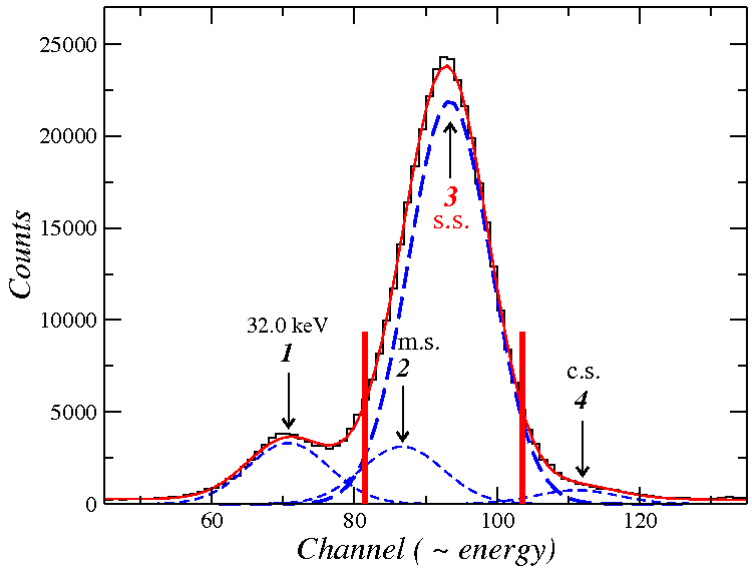

Fig. 3 – Example of gaussian peak decomposition of a scattered spectrum in the geometry of Fig. 1. The peaks have the following energies: no. 1: 32 keV; no. 2: 45.0 keV; no. 3: 48.7 keV (the single Compton scattering peak); no. 4: 58 keV. The two markers show the limits of the peak integration discussed in the text.

It can be seen that there are four peaks in this region. Peak 1 is the 32 keV line; peak 2 which can be seen as a tail on the left side of the big peak; peak 3 which is the one-scattering peak; and a small peak 4 at the right. Fig. 3 shows a fit of the spectrum by treating all these peaks as gaussians. Peak 3 has an energy of 48.7 keV and a FWHM resolution of 6.7 keV, both corresponding well to the expected central value of 48.9 keV (for $\theta \approx 150^0$) and an increased effective resolution. Peak 4 has about the energy of the incident gamma rays, therefore we assign it to the coherent scattering. Peak 2, with a energy of 45.0 keV is interpreted as due to multiple-scattering events that reach the detector; it is likely that it corresponds mostly to two-three scatterings. The photons reaching the detector after more scatterings will have less and less average energy in the spectrum. The 32 keV peak from spectra measured during the same time, and for different contents of water in the brick (this will be discussed later) is found with an intensity that is not constant as expected, but increases slightly with increasing water content, suggesting that the peak we fit in that position contains contribution from multiple scatterings (another indication that this is the case is its increased width, of 6.7 keV). We do not know the exact shape of the spectrum due to the multiple-scattered photons, but the two- and three-fold scattering events must have in average several keV less than the one-scattering events (peak 3), therefore the spectrum decomposition shown in Fig. 3 is a reasonable procedure for

disentangling the single-scattering events from the multiple-scattering ones. One can also see from Fig. 2 that in the case of the "100^0" geometry the contribution of the multiple scattering is bigger, the left side tail of peak 3 almost covering the 32 keV peak.

Before presenting the actual measurements, let us consider *what is measured*. By comparing a dry brick with one in which a certain amount of water was absorbed, we see the effect from Fig. 2, which is, in essence, due to an increase of the density of the brick. The measured effect can be assigned only to the added water if the material is highly homogeneous, that is, we do not find pieces of material (different bricks) of different densities. In our case the measured density of the bricks was found constant with a good accuracy. In general, this is hopefully valid for all the pieces of a given batch fabricated in the same conditions. Second, as emphasized in the introduction, the building materials are porous materials, which allow water circulate freely inside by capillarity forces, that is, after some time the water will be uniformly distributed in the material [2] (if the porosity of the material is also uniformly distributed). This was also proved by the results of measurements performed at different locations on the brick, as it will be discussed later. Under such conditions we may state that the effect we see can be interpreted in terms of an average moisture content, which should be the same when measured at any point within the material. Of course, if the gamma ray beam would hit a region where there is an intrusion of a denser material, we would see a similar effect, but this can hopefully be discerned by measuring the material in several points.

3. MEASUREMENTS AND RESULTS

After demonstrating the effect of the added humidity, measurements were performed to calibrate the method, that is, to find the relationship between the measured effect and the actual water content of the bricks. Bricks for these measurements were chosen at random from the same batch, the only condition was that their shape is regular such that their sizes can be measured accurately. Their density, calculated from the measured mass and sizes, was found to coincide within ±3%, the average value deduced being 1.58 ± 0.04 g/cm^2. Six of these bricks were used for the calibration procedure. It was initially checked that the scattering spectra measured in the geometry of Fig. 1, during identical time intervals, and with the gamma ray beam hitting different locations, are essentially identical for all these bricks, a fact which confirmed the homogeneity of the material. The linear attenuation coefficient for the 59.5 keV radiation (measured by transmission of a collimated beam through the brick thickness of 6 cm) was found 0.40 ± 0.01 cm^{-1}. One of these bricks was kept "dry", as a reference, and the other five were loaded with different water quantities. The procedure was to absorb a certain quantity of water in each brick (of known mass) by pouring small quantities on all its faces,

then let it 24 hours such that the absorbed water distributed itself uniformly by capillarity, and weigh the brick again before the measurement. One of the five bricks was saturated with water by storing it under water. For each brick we define the moisture content as:

$$U = \frac{M_{\text{wet}} - M_{\text{dry}}}{M_{\text{wet}}}, \tag{2}$$

where M_i is the mass of the brick in the indicated state. Each brick was then measured in the geometry of Fig. 1, with a counting time of 10 minutes. For each brick, two measurements were performed, with the incident gamma ray beam irradiating two regions chosen at random on different faces of the brick. In each case we found a good agreement between the two measurements, attesting again the fact that we measured domains with the same composition and water content. This procedure was necessary in order to avoid possible insertions of a different composition in the irradiated volume, as well as to test the uniformity of the water distribution within the material. From the comparison with the reference spectrum (measured for the dry brick) we extracted the measured effect E:

$$E = \frac{C_{\text{wet}} - C_{\text{dry}}}{C_{\text{dry}}}, \tag{3}$$

where C_i is the number of counts in the single-scattering gamma ray peak in the specified state. Two procedures were used to extract the area of the single-scattering peak. One is the fitting of four gaussian peaks in the region comprising this peak, as illustrated in Fig. 3, in which peak 3 is the one of interest. The second was a simple integration of this peak between the markers shown in Fig. 3 (channels 82 to 103). With the later procedure we get rid of the contributions of the 32 keV line and of the coherent scattering, but some contribution from events with more than one scattering still remains.

Table 1 presents the results of these two procedures. Figure 4 shows the correlation between the humidity U and the measured effect E. The observed dependence can be well approximated in each case by a linear one. The curves passed through the data points are fits with straight lines constrained to pass through the origin: $E = aU$. It is seen that in the case when the gaussian peak fitting was used to extract the intensity of the one-scattering peak the effect is practically $E = U$ (slope of the fitted straight line close to 1), and larger than in the case when the largest portion of the peak was simply integrated (slope around 0.8). It is clear that not disentangling the single-scattering events from events with more than one scattering worsens the response effect. One should emphasize that these moisture measurements are not absolute, because we used as reference a ”dry” brick, that is, a brick with an unknown equilibrium humidity (which under normal conditions may stabilize at a value of about 3% [1]).

Table 1

The measured effect calculated with eq. (3), versus different moistures as determined with eq. (2). The experimental values represent the average of two different measurements as explained in the text. The reference for calculating the *U* and *E* values was the "dry" brick, which may have, nevertheless, some intrinsic humidity (in equilibrium with the air in the room)

Brick nr.	*U* (%)	*E* (%) [peak fit]	*E* (%) [peak integration]
1	12.82	14.39 ± 1.69	10.62 ± 0.19
2	11.39	11.04 ± 1.57	8.18 ± 0.66
3	8.59	6.98 ± 1.68	6.16 ± 0.54
4	6.22	6.67 ± 2.11	5.52 ± 0.51
5	3.67	3.93 ± 1.86	2.75 ± 0.46

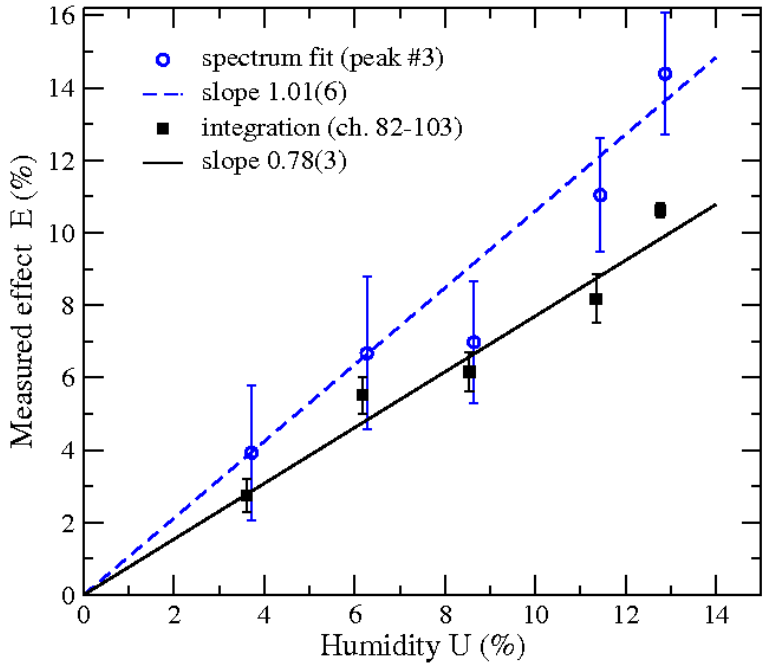

Fig. 4 – Correlation between the moisture conten *U* and the measured effect *E*. The quantity *E* was deduced in two ways (Table 1): a) evaluation of the single-scattering interaction by peak fitting (as in Fig. 3) – circles; b) integration of the spectrum in the region of this peak (between the two markers in Fig. 3) – squares. The two sets of experimental data are drawn at slightly different abscissas in order to distinguish the error bars. The errors result from those of the peak fitting procedure in case a), and from the statistical errors in case b). The curves are straight lines with the given slopes fitted to the data.

In Fig. 5 we show a comparison of the measurements from Fig.4 with those of another measurement, performed under the same geometrical conditions, on a different set of six bricks from the same batch, but with counting times of only

2 minutes per point. The two sets of measurements give very similar results, a straight line fit to all points providing the result $E = (1.09 \pm 0.13)U$.

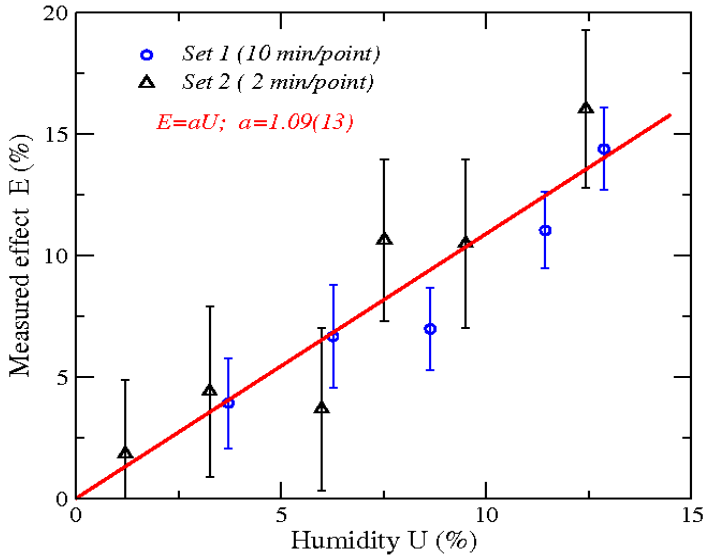

Fig. 5 – Comparison between two sets of measurements on the same type of bricks: the one from Fig. 4 (measuring time 10 min/point) and another one with 2 min/point. The line is the fit to all 11 data points.

In the following we make a simple estimation of the expected magnitude of the effect E. Consider Compton scattering that takes place around a point of the gamma-ray beam situated at a distance x inside the brick, and is detected at an angle θ (Fig. 1). This would correspond to a strong collimation of both the source and the detector. The intensity detected for the Compton scattered radiation in the case of the material without water is

$$I_c = I_0 C_i V D_e \mathrm{e}^{-\mu_i x} \mathrm{e}^{-\mu_f x/|\cos\theta|} + \mathrm{m.s.}, \tag{4}$$

where I_0 is the intensity of the incident beam, i and f refer to the initial and final (scattered) energy of the photon, respectively; μ are the linear attenuation coefficients; C_i is a constant that includes a solid angle factor, the detection efficiency, and the Compton scattering cross-section per electron; V is the inspected volume (in this case a small volume around the point at x); D_e is the density of electrons inside the volume V; *m.s.* refers to a possible contribution from multiple scattering. The two exponentials reflect the attenuation of the incident radiation along the path x within the object, and of the scattered radiation in the same material on its way towards the detector. For the wet object we have

$$I_{c(wet)} = I_0 C_i V D_{e(wet)} e^{-\mu_{i(wet)} x} e^{-\mu_{f(wet)} x/|\cos\theta|} + \text{m.s.} \quad (5)$$

The attenuation coefficient of the wet object can be calculated from those of the dry object, μ, and of the water, μ_w, by using the Bragg's law and the definition of eq. (3) for the moisture U:

$$\mu_{(wet)} = \mu + \mu_w \frac{U}{1-U} \frac{\rho}{\rho_w}, \quad (6)$$

where ρ and ρ_w are the mass density of the dry object and of the water, respectively. One has taken into account that after absorption of water in building materials (such as the brick) the initial volume is kept: the material neither swells, nor shrinks. The densities of electrons (the number of electrons per unit of volume) can be calculated, for a compound, as $\rho_e = \frac{\rho}{u} \sum w_i \frac{Z_i}{A_i}$, where u is the atomic mass unit, and Z_i, A_i are the number of electrons and the mass number of the i^{th} component with the weight factor w_i. The usual composition of a clay brick includes different proportions of SiO_2, Al_2O_3, (usually predominant), and Fe_2O_3, CaO, MgO, Na_2O [14]. Independent of their proportions, we get for the dry brick a value very close to

$$D_e = 0.5 \frac{\rho}{u}. \quad (7)$$

For the wet object (H_2O added in the proportion U) one gets

$$D_{e(\text{wet})} = (0.5 + \frac{10}{18} \frac{U}{1-U}) \frac{\rho}{u}. \quad (8)$$

Assume now that we measure at the surface of the object ($x \approx 0$) where the attenuations and the multiple scattering can be neglected. Then, from (3), (4), (5), we have:

$$E(x \approx 0) = \frac{I_{c(\text{wet})}}{I_c} - 1 = \frac{D_{e(\text{wet})}}{D_e} - 1 = 1.111 \frac{U}{1-U}. \quad (9)$$

This is the largest effect that one can measure for a given U, which, for small values of U, is $E \approx 1.111U$.

For a given, finite x, the value of the effect E calculated in the same way will be reduced due to the attenuation factors in (4) and (5). In the real case, when one measures with a broader collimation of the detector, or with the uncollimated detector (Fig. 1), one has to integrate the intensities (4) and (5) over all values of x and all values of the angle θ allowed by the geometry, and then calculate E from the ratio of the two integrals. The best way to do this is by a Monte Carlo approach

which must take into account other effects as well: the variation of the Compton scattering cross section with the angle θ; the variation of the attenuation coefficient μ_f (which is determined by both Compton scattering and photoelectric effect cross sections) with the energy of the scattered photon, that is, with θ; multiple scattering. We finally mention that the coherent scattering peak (nr. 4 in Fig. 3) could be also used, in principle, to the characterization of the material (see ref. [34]), but in our case the intensity of this peak was too small and unreliably extracted.

4. CONCLUSIONS

The results of this work show that the measurement of the Compton backscattering of the 59.5 keV gamma rays from a ^{241}Am source represents a useful, non-destructive technique for measuring the moisture content within porous building materials, such as the common fired-clay brick. With a very simple geometry the obtained scattering signal (or measured effect E) was reasonable: $E \approx U$. This measurement represents a bulk sample, because the detector was not collimated. It was shown that even in this case one can use a 'soft' collimation and ensure in this way that we measure mostly single-scattering events. The measured effect is strongest when we use this soft collimation (that is, a decomposition of the spectrum in the scattered peak region by a fit with gaussian peaks). One may think that this kind of spectrum processing is too complicated to be used by non-specialized people. However, with a reasonable stability of the measuring electronic chain, the peak fitting procedure in the region of interest can be programmed and performed in an automatic way. In this way, it is even more stable and reliable than the apparently simpler method of the peak integration, which may suffer from instabilities of the electronics. In principle, if we collimate tightly both the source and the detector, we are able to probe the humidity at different depths. On the other hand, this means a reduction of the counting rates, therefore for reasonably short measuring times one needs stronger sources, which, in turn, require more massive protection. These measurements are relative, in the sense that a reference is needed. Also, a calibration is necessary. In practical situations, we choose the reference by measuring in a region considered to be "dry". Even if we do not know, a priori, such a point, one can map with measurements the desired region and then refer everything to the point found with minimum moisture, and use a calibration line like that in Fig. 4 to deduce relative moisture contents. One should emphasize again, however, that what we measure with this method is a variation in density, which can be interpreted as due to moisture only if the material measured is highly homogenous, which may be rarely the case in practical situations.

Further developments of this method are possible. For practical applications, more determinations are necessary for different other building materials. Also, the geometry (average scattering angle, a better definition of the interaction volume)

can be optimized. The results of such measurements could be quantitatively understood by a Monte Carlo modeling of the Compton scattering processes in given experimental conditions (both geometry and composition of the scatterer). In order to better understand and characterize the multiple scattering in the geometry used by us, we plan measurements in which a HPGe detector will be used in parallel to the $LaBr_3$ detector. For field applications, one can further increase the compactness of the apparatus by still reducing its size and weight. This is possible by using a weaker source (e.g., a few hundreds of μCi), with a correspondingly smaller protection. In addition, one may take advantage of fully integrated multichannel analyzer systems offered commercially, that contain everything needed to support a scintillator detector spectroscopy system, in a tube base powered from the USB port of a laptop. In this way the system becomes more suitable for field measurements.

REFERENCES

1. S.F. Musso, *Recupero e restauro degli edifici storici,* EPC Libri s.r.l., Rome, 2004.
2. C. Hall and W. Hoff, *Water transport in brick, stone, and concrete*, Spon Press, London, 2002.
3. E.M.A. Hussein, *Handbook on radiation probing, gauging, imaging and analysis,* Kluwer Academic Publishers, Dordrecht, 2003.
4. H. Pleinert, Sadouki, and F.H. Wittmann, Materials and Structures, **31**, 218–224 (1998).
5. J. Obhodaš, D. Sudac, K. Nad, V. Valković, G. Nebbia, and G. Viesti, Nucl. Instr. Meth. Phys. Res., **B 213**, 445–451 (2004).
6. R.J. Gummerson, C. Hall, W.D. Hoff, R. Hawkes, G.N. Holland, and W.S. Moore, Nature, **281**, 56–57 (1979).
7. L. Pel , K. Kopinga, G. Bertram, and G. Lang, J. Phys., **D 28,** 675–680 (1995).
8. G. Knoll, *Radiation detection and measurement*, John Wiley & Sons, 2000.
9. C.G. Gurr, Soil Science, **94**, 224–229 (1962).
10. P.H. Groenevelt, J.G. de Swart, and J. Cisler, Bull. Int. Assoc. Sci. Hidrology, **XIV**, 67–788 (1969).
11. B.D. Soane, Nature, **214**, 1273–1274 (1967).
12. J.C. Corey, S.F. Peterson, and M.A. Wakat, Soil Sci. Soc. Amer., **35**, 215–219 (1971).
13. M.E. Medhat, Ann. Nucl. Energ., **36**, 849–852, (2009).
14. I.C.P. Salinas, C.C. Conti, and R.T. Lopes, Appl. Rad. Isot., **64**, 13–18 (2006).
15. M.I. Awadallah, and M.A.Imran, J. Environ. Rad., **94**, 129–136 (2007).
16. C. Singh, T. Singh, A. Kumar, and G.S. Mudahar, Ann. Nucl. En., **31**, 1199–1205 (2004).
17. R. Meckbach, P. Jacob, H.G. Paretzke, Nucl. Instr. Meth. Phys. Res., **A 255** 160–164 (1987).
18. I. Akkurt, S. Kilincarslan, and C. Basuigit, Ann. Nucl. En., **31**, 577–582 (2004).
19. H.M. Morgan, J.T. Shakeshaft, and S.C. Lillicrap, Appl. Rad., Isot., **49**, 555–557 (1998).
20. R.S.Holt, M.J. Cooper, and D.F. Jackson, Nucl. Instr. Meth. Phys. Res., **221**, 98–104 (1984).
21. E.M.A. Hussein, and T.M. Whynot, Nucl. Instr. Meth. Phys. Res., **A 283**, 100–106 (1989).
22. S. Tuzi, and O. Sato, Appl. Rad. Isot., **44**, 1279–1284 (1993).
23. R.T. Lopes, C.M. Valente, E.F.O. De Jesus, and C.S. Camerini, Appl. Rad. Isot., **48**, 1443–1450 (1997).
24. B. Bridge, J.M. Gunnell, D.C. Imrie, and N.J. Olson, Nondestructive Testing Communications, **2**, 103–113 (1986).
25. A.M. Yacout, M.H. Van Haaren, and W.L. Dunn, Appl. Rad. Isot., **48**, 1313–1320, (1997).
26. W.L. Dunn, and A.M. Yacout, Appl. Rad. Isot., **53**, 625-632 (2000).
27. M.J. Anjos, R.T. Lopes, and J.C. Borges, Nucl. Instr. Meth. Phys. Res., **A 280**, 535–538, (1989).

28. M.J. Aguiar, C.J.G. Carneiro, A.H. Oliveira, R. Penna, and M.R.S. Silva, *Int. Nuclear Atlantic Conf. – INAC 2007, Santos, Brazil XV ENFIR, VIII ENAN – Nuclear Energy and Energetic Challenges for 21st Century*, v. ´UNICO (2007), pp. 159–163.
29. O. Ciftcioglu, and D. Taylor, Nucl. Instr. Meth. Phys. Res., **94**, 53–59 (1971).
30. O. Ciftcioglu, D.A. Byatt, and D. Taylor, J. Soil Sci., **23**, 32–27 (1972).
31. C. Ertek, and N. Haselberger, Nucl. Instr. Meth. Phys. Res., **227**, 182–185 (1984).
32. P.R. Menge, G. Gautier, A. Iltis, C. Rozsa, and V. Solovyev, Nucl. Instr. Meth. Phys. Res., **A 579**, 6–10 (2007).
33. D. Alexiev, K. Mo, D.A. Prokopovich, M.L. Smith, and M. Matuchova, IEEE Trans. Nucl. Sci., **55**, 1174 (2008).
34. J.R. Mossop, S.A. Kerr, D.A. Bradley, C.S. Chong, and A.M. Ghose, Nucl. Instr. Meth. Phys. Res., **A 255**, 419–422 (1987).